

Delay Embedded Echo-State Network: A Predictor for Partially Observed Systems

Debdipta Goswami*

* *Department of Mechanical and Aerospace Engineering, The Ohio State University, Columbus, OH 43210 USA (e-mail: goswami.78@osu.edu).*

Abstract: This paper considers the problem of data-driven prediction of partially observed systems using a recurrent neural network. While neural network based dynamic predictors perform well with full-state training data, prediction with partial observation during training phase poses a significant challenge. Here a predictor for partial observations is developed using an echo-state network (ESN) and time delay embedding of the partially observed state. The proposed method is theoretically justified with Taken's embedding theorem and strong observability of a nonlinear system. The efficacy of the proposed method is demonstrated on three systems: two synthetic datasets from chaotic dynamical systems and a set of real-time traffic data.

Keywords: Nonlinear system identification, Neural networks, Observability, Chaotic attractor, Machine learning, Reservoir computer

1. INTRODUCTION

The ongoing quest of modeling complex systems from data has motivated a wide array of machine learning techniques proving their utility in a variety of problems, e.g., classification, speech recognition (Hinton et al. (2012)), board games (Silver et al. (2016)), and even discovering mathematical algorithms (Fawzi et al. (2022)). There has been a renewed interest in data-driven prediction of dynamical systems in the past decade where recurrent neural networks (RNN) played a central role. For example, an echo-state network (ESN) proposed by Jaeger and Haas (2004) can model chaotic systems with great effect (Lu et al. (2017), Pathak et al. (2018)). However, these prediction techniques need full-state data for training and rely on the underlying dynamic structure to approximate the state-transition map to predict a dynamical system. But in many practical cases, only a partial observation is available during the training phase. Such applications include fluid flow structure, atmospheric dynamics, and traffic data.

Neural network predictors, instead of using a handcrafted dynamic model from the physics of the system, utilize a set of training data to update a parametric surrogate model, and then employ it to predict future states. They implicitly assume that all the relevant variables are adequately represented in the training dataset and hence, require full state measurement for proper training. Although Lu et al. (2017) and Goswami et al. (2021) developed ESN-based methods to utilize sparse partial measurements for predicting unmeasured variables in the testing phase, these require full-state data for training.

An ESN uses a reservoir of nonlinear, randomly firing neurons to process time-varying input signal. Such a reservoir with a convergence property, known to the ESN literature as echo-state property (ESP) can uniformly approximate

any nonlinear fading memory filter as proved in Grigoryeva and Ortega (2018). The attractiveness of an ESN as a neural engine of a predictor is that any convergent reservoir dynamics can be tuned via output connections (also called the readout map) with minimal computing resources. Also, Tanaka et al. (2019) and Nakajima and Fischer (2021) describe hardware implementations of the reservoir using field programmable gate arrays (FPGAs) or a photonic reservoir, thereby increasing efficiency and reducing computational overhead. It is also extended to quantum computing realm via quantum reservoir computers (QRCs) as shown in Fujii and Nakajima (2017) and Chen et al. (2019). Lu et al. (2017), Goswami et al. (2021), and Goswami et al. (2022) describe the effectiveness of ESN-based approaches for sparse estimation of chaotic systems and traffic network prediction.

This paper develops an ESN-based predictor for systems with partial measurements available for network training. The proposed method utilizes the universal approximation property of a fading memory ESN (Grigoryeva and Ortega (2018)) coupled with Taken's embedding theorem (Takens (1981)) to determine a dynamic map that predict the future values of the partial observation. Takens (1981) showed that a time series of typical scalar measurements can faithfully reconstruct the attractor set of a chaotic dynamical system. This result motivates the utilization of a delay embedded partial measurements to train the ESN as a dynamic map for next step prediction. It is further proved for a general nonlinear system that a finite time observability condition on an open set is sufficient for existence of such a dynamic map.

The contribution of this paper are (1) providing a data-driven predictor for partial observations from a higher dimensional nonlinear systems via ESN; (2) utilization of Taken's embedding theorem and strong observability

condition to guarantee the existence of such dynamic predictor; (3) application of the prediction method on a real set of mobility data in order to forecast traffic volume in a road network.

This paper is organized as follows. Section 2 provides a brief overview of the echo-state network (ESN). Section 3 presents the ESN algorithm with delay embedded input and provide theoretical justification of the algorithm. Section 4 illustrates the applications to three different problems: two synthetic data streams generated by chaotic nonlinear systems and one real set of traffic sensor data. An ablation study with different embedding dimension is also provided. Section 5 concludes the manuscript and discusses ongoing and future work.

2. ECHO-STATE NETWORKS: DYNAMICAL SYSTEM PREDICTOR

Echo-state networks (ESN) are a special kind of recurrent neural network used for the prediction of dynamical systems and time-series. It consists of a large, randomly connected reservoir of neurons driven by the input signal. The nonlinear response signals thus induced in the neurons are then linearly combined to match a desired output signal. This technique is also known as reservoir computer (RC) (Maass and Markram (2004)). An ESN consists of an input layer $\mathbf{u} \in \mathbb{R}^m$, coupled through input coupling matrix $W_{in} \in \mathbb{R}^{n \times m}$ with a recurrent nonlinear reservoir $\mathbf{r} \in \mathbb{R}^n$. The output $\mathbf{y} \in \mathbb{R}^p$ is generated from n neurons of the reservoir via a readout matrix $W_{out} \in \mathbb{R}^{n \times p}$. The reservoir network evolves nonlinearly in following fashion (Maass and Markram (2004), Goswami et al. (2021))

$$\mathbf{r}(t + \Delta t) = (1 - \alpha)\mathbf{r}(t) + \alpha\psi(W\mathbf{r}(t) + W_{in}\mathbf{u}(t)). \quad (1)$$

The time-step Δt is chosen according to the sampling interval of the training data. The leakage rate parameter $\alpha \in (0, 1]$ slows down the evolution of the reservoir as $\alpha \rightarrow 0$. The nonlinear activation function ψ is usually a sigmoid function, e.g., $\tanh(\cdot)$ or a logistic function. The output depends linearly on the reservoir states (Maass and Markram (2004), Goswami et al. (2021)), i.e.,

$$\mathbf{y}(t) = W_{out}\mathbf{r}(t). \quad (2)$$

The weights W_{in} and W are initially randomly drawn and then held fixed. The weight W_{out} is adjusted during the training process. The reservoir weight matrix W is usually kept sparse for computational efficiency.

An ESN is trained by driving it with an input sequence $\{\mathbf{u}(1), \dots, \mathbf{u}(N)\}$ that yields a sequence of reservoir states $\{\mathbf{r}(1), \dots, \mathbf{r}(N)\}$. The reservoir states are stored in a matrix $\mathbf{R} = [\mathbf{r}(t_1), \dots, \mathbf{r}(t_N)]$. The correct outputs $\{\mathbf{y}(1), \dots, \mathbf{y}(N)\}$, which are part of the training data, are also arranged in a matrix $\mathbf{Y} = [\mathbf{y}(1), \dots, \mathbf{y}(N)]$. The training is carried out by a linear regression with Tikhonov regularization as follows (Jaeger and Haas (2004)):

$$W_{out} = \mathbf{Y}\mathbf{R}^T(\mathbf{R}\mathbf{R}^T + \beta\mathbf{I})^{-1}, \quad (3)$$

where $\beta > 0$ is a regularization parameter that ensures non-singularity.

Remark 1. An ESN is a universal approximator, i.e., it can realize every nonlinear operator with bounded memory arbitrarily accurately, if it satisfies the echo state property (ESP) as explained in Jaeger and Haas (2004). The ESP

states that the reservoir will asymptotically wash out any information from the initial conditions. For the $\tanh(\cdot)$ activation function, Jaeger and Haas (2004) empirically observed that the ESP holds for any input if the spectral radius of W is smaller than unity. To ensure this condition, W is normalized by its spectral radius.

3. DELAY EMBEDDED ECHO-STATE NETWORK: A PREDICTOR FOR PARTIAL SCALAR OBSERVATION

An ESN can be trained to predict a time-series $\{\mathbf{x}_i \in \mathbb{R}^d : i \in \mathbb{N}\}$ generated by a dynamical system by setting $\mathbf{u}(t)$ and $\mathbf{y}(t)$ as the current and next state value (i.e., \mathbf{x}_k and \mathbf{x}_{k+1}) respectively. The network is trained for a certain training length N of the time-series data $\{\mathbf{x}_i, i = 1, \dots, N\}$, and then can run freely by feeding the output \mathbf{y}_k back to the input \mathbf{u}_{k+1} of the reservoir. In this case, both \mathbf{u} and \mathbf{y} have the same dimension d as that of the time-series data.

An ESN proves to be a powerful tool for dynamical systems prediction when trained with full-state data as demonstrated in Lu et al. (2017) and Pathak et al. (2018). Goswami et al. (2021) improves its performance by assimilating partial observations during the testing phase through an ensemble Kalman filter. However, a significant challenge is posed when only a partial scalar measurement $\{x_i \in \mathbb{R} : i \in \mathbb{N}\}$ of the state is available during the training phase. A simple approach is to treat the scalar measurements as a separate time-series and use it to train an ESN Fig. 1 (b). The trained ESN can then be used to predict the future values of the scalar time series $\{x_i \in \mathbb{R} : i = N + 1, \dots\}$. But this simplistic approach disregards the fact that the scalar time series comes from a high dimensional system and the next step prediction x_{k+1} of the scalar observable might depend on not only x_k but its previous values $x_{k-(m-1)}, \dots, x_k$ via higher dimensional embedding.

This paper proposes an alternative method of partial state prediction by utilizing time delay embedding in conjunction with an ESN. This approach is inspired by Takens (1981) and Sauer et al. (1991) which show that the time-delay embedding of a scalar measurement time-series can diffeomorphically reconstruct the strange attractor of the original dynamics. This result is famously stated as Taken's embedding theorem:

Theorem 1. Let a discrete-time dynamical system $\mathbf{x}_{k+1} = f(\mathbf{x}_k)$ is given by a smooth map $f : \mathbb{X} \rightarrow \mathbb{X}$ on a d dimensional manifold $\mathbb{X} \in \mathbb{R}^d$. Assume that the dynamics evolve on a strange attractor A with a box-counting dynamics d_A . Then A can be embedded in \mathbb{R}^m with $m > 2d_A$, i.e., \exists a diffeomorphism $\phi : A \rightarrow \mathbb{R}^m$ such that the derivative of ϕ is full rank. Moreover, let $h : \mathbb{X} \rightarrow \mathbb{R}$ be a smooth scalar observation function with full rank derivative and no special symmetry in the component. Then the function $e : \mathbb{X} \rightarrow \mathbb{R}^m$ defined as

$$e(\mathbf{x}) \triangleq (h(\mathbf{x}), h(f(\mathbf{x})), \dots, h(f^{m-1}\mathbf{x}))$$

is an embedding of A in \mathbb{R}^k .

Proof. See Takens (1981). ■

The embedding is demonstrated in Fig. 2. Since the

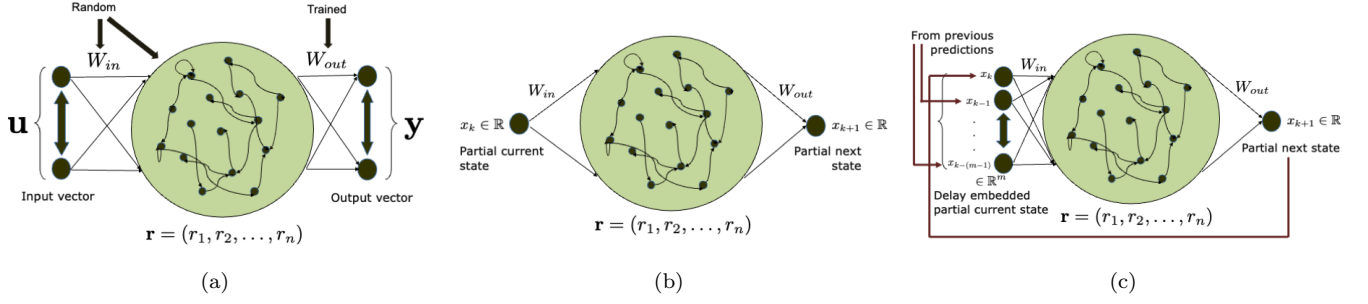


Fig. 1. Architecture of an EnKF-ESN: (a) the basic ESN, (b) an ESN for scalar partial state prediction, and (c) a delay-embedded ESN for partial state prediction

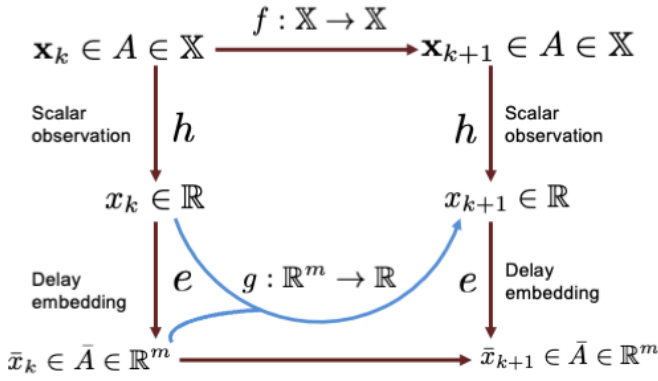


Fig. 2. Schematic of the Takens embedding theorem (Vlachos and Kugiumtzis (2008))

scalar measurements $\{x_i : i \in \mathbb{N}\}$ can be delay embedded to an attractor \bar{A} diffeomorphic to A , there is a map $g : \mathbb{R}^m \rightarrow \mathbb{R}$ to the next step scalar observation x_{k+1} from the time-delay embedding of its previous values $\{x_k, \dots, x_{k-m+1}\}$. This result, coupled with the universal approximation property of an ESN Grigoryeva and Ortega (2018), provides a strong basis to use delay embedding for the input layer in order to predict the partial scalar observation (Fig. 1(c)). Algorithm 1 presents the procedure for training an ESN using delay-embedded scalar measurements. The inputs are taken as vectors $\bar{x}_k = [x_k, \dots, x_{k-m+1}]^T$ of m delayed observations. The ESN is trained with next step scalar observation x_{k+1} as outputs.

Remark 2. The condition of full rank derivative and no special symmetry on the observation function h is important and closely relates to the notion of observability of a nonlinear system.

Remark 3. The embedding dimension m , as specified in Theorem 1, is at most $2d + 1$, but it can be often less in reality. For example, Lorenz system yields a theoretical value of $m = 5$ for because its strange attractor has a box-counting dimension $d_A = 2.06 \pm 0.01$. For a delay-embedded ESN (Fig. 1(c)), m is a hyperparameter that needs to be tuned for the best performance.

Remark 4. While Taken's embedding theorem is valid for systems with strange attractors, the delay embedded ESN can be used for any strongly observable nonlinear system on its domain of observability as will be shown next.

This method is also suited for quasi-periodic systems as demonstrated in this paper.

Algorithm 1 Training a delay-embedded ESN

Input: Training scalar measurements $\{x(1), \dots, x(N)\}$
Hyperparameters: Delay embedding dimension m , Training length N , leaking rate α , regularization parameter β , reservoir connection probability $p \in (0, 1)$, reservoir size n , activation ψ
Output: W_{in}, W, W_{out}

```

procedure TRAIN(  $\{x(1), \dots, x(N)\}; m, \alpha, \beta, p, n, \psi$  )
  Generate  $W \sim G(n, p)$   $\triangleright$  Adjacency matrix of an
  Erdős-Renyi random graph
  Generate  $W_{in} \in \mathbb{R}^{n \times m}$  random matrix
   $\bar{x}(i) \leftarrow [x(i), x(i+1), \dots, x(i+m-1)]^T$ 
   $\forall i \in 1, \dots, N-m$   $\triangleright$  Delay embedding
   $\mathbf{Y} \leftarrow [x(m+1), x(m+2), \dots, x(N)]$   $\triangleright$  Arrange
  outputs
   $\mathbf{r}_1 \leftarrow \mathbf{0}_n$   $\triangleright$  Initialize reservoir
  for  $i = 1$  to  $N-m$  do
     $\mathbf{r}(i+1) \leftarrow (1-\alpha)\mathbf{r}(i) + \alpha\psi(W\mathbf{r}(i) + W_{in}\bar{x}(i))$ 
  end for
   $\mathbf{R} \leftarrow [\mathbf{r}(1), \dots, \mathbf{r}(N-m)]$   $\triangleright$  Arrange reservoir states
   $W_{out} \leftarrow \mathbf{Y}\mathbf{R}^T(\mathbf{R}\mathbf{R}^T + \beta\mathbf{I})^{-1}$   $\triangleright$  Train output weights
end procedure

```

A time-series of partial observation $\{x_1, \dots, x_N\} = \{h(\mathbf{x}_0), h^2(f(\mathbf{x}_0)), \dots, h(f^{N-1}(\mathbf{x}_0))\}$ from a dynamical system $\mathbf{x}_{k+1} = f(\mathbf{x}_k)$ with an observation function $h(\cdot)$ is able to predict the next step by training an universal functional approximator if the observability condition is satisfied as stated below.

Definition 1. (Nijmeijer (1982)) Consider an autonomous discrete-time nonlinear system

$$\begin{aligned} \mathbf{x}_{k+1} &= f(\mathbf{x}_k) \\ y_k &= h(\mathbf{x}_k), k \in \mathbb{N} \cup \{0\}, \end{aligned} \quad (4)$$

where $f : \mathbb{X} \subset \mathbb{R}^d \rightarrow \mathbb{X}$ and $h : \mathbb{X} \rightarrow \mathbb{R}$ are smooth functions defined on an open subset $\mathbb{X} \subset \mathbb{R}^d$. The system (4) is said to be *strongly observable*, or *finite-time observable* if for any $\mathbf{x}, \tilde{\mathbf{x}} \in \mathbb{X}$,

$$\begin{bmatrix} h(\mathbf{x}) \\ h(f(\mathbf{x})) \\ \vdots \\ h(f^{d-1}(\mathbf{x})) \end{bmatrix} = \begin{bmatrix} h(\tilde{\mathbf{x}}) \\ h(f(\tilde{\mathbf{x}})) \\ \vdots \\ h(f^{d-1}(\tilde{\mathbf{x}})) \end{bmatrix}$$

implies $\mathbf{x} = \tilde{\mathbf{x}}$.

Table 1.

Hyperparameter	Value		
	Lorenz system (5)	Rössler system (7)	Traffic Volume
Reservoir size n	500	500	4000
Reservoir connection probability p	0.01	0.01	0.01
Training length N	1000	1000	1000
Activation $\psi(\cdot)$	$\tanh(\cdot)$	$\tanh(\cdot)$	$\tanh(\cdot)$
Leaking rate α	0.3	0.3	0.7
Regularization β	10^{-6}	10^{-6}	10^{-6}

For this paper, we assume the observation y_k are partial state x_k .

Theorem 2. Consider a scalar time series $\{x_i : i \in \mathbb{N} \cup \{0\}\}$ observed from a nonlinear dynamics (4) with a full state history $\{\mathbf{x}_i : i \in \mathbb{N} \cup \{0\}\}$, and observation function $h(\cdot)$ such that $y_k = x_k = h(\mathbf{x}_k)$. If the system (4) is strongly observable, then there is a continuous map $g : \mathbb{R}^d \rightarrow \mathbb{R}$ from a delay-embedded partial state observation $\bar{x}_k = [x_k, \dots, x_{k-d+1}]$ to the next step x_{k+1} . Moreover, there exists an ESN, properly chosen, that can approximate g arbitrarily accurately.

Proof. Let $\mathbb{Y} \subset \mathbb{R}^d$ be the set of all possible d -step observation sequence, i.e., $\mathbb{Y} = [h, h \circ f, \dots, h \circ f^{d-1}](\mathbb{X})$. The strong observability condition in Definition 1 states the existence of a bijection $H(\cdot) \triangleq [h, h \circ f, \dots, h \circ f^{d-1}](\cdot)$ from \mathbb{X} to \mathbb{Y} . Now since H is smooth (i.e., at least continuously differentiable) by construction on an open set \mathbb{X} , $\mathbb{Y} = H(\mathbb{X})$ is also open in \mathbb{R}^d and H is a homeomorphism between \mathbb{X} and \mathbb{Y} . Hence, H has a continuous inverse $G : \mathbb{Y} \rightarrow \mathbb{X}$ which maps the delay-embedded observation sequence $\bar{x}_k = [x_k, \dots, x_{k-d+1}]$ to \mathbf{x}_{k-d+1} . Now according to the dynamics (4), $x_{k+1} = h \circ f^d(\mathbf{x}_{k-d+1})$ with smooth $h \circ f^d$. Therefore, we can construct a continuous function $g : \mathbb{Y} \subset \mathbb{R}^d \rightarrow \mathbb{R}$ such that $g \triangleq h \circ f^d \circ G$. The last part of the theorem is a direct result of Theorem 4.1 in Grigoryeva and Ortega (2018) which proves the universality of an ESN. ■

Remark 5. Although *strong observability* is assumed in Theorem 2, a weaker condition of *strong local observability* (Nijmeijer (1982)) suffices for most nonlinear systems in practice. A system (4) is *strongly locally observable* at a point $\mathbf{x} \in \mathbb{X}$ if the strong observability condition is satisfied in a neighborhood U of \mathbf{x} .

Remark 6. With the strong observability assumption, the embedding dimension m should equal the system state dimension d . But in practical implementations, m needs to be tuned to get the best performance.

4. NUMERICAL PERFORMANCE

This section illustrates the performance and ablation study of a delay embedded ESN on three prediction problems from partial state data. The first two are time-series generated by chaotic dynamical systems and the last one is a real-time traffic flow data obtained by Numina sensor nodes (Numina (2019)) installed on the University of Maryland campus.

4.1 Lorenz System

The delay-embedded ESN is tested on a time-series generated by the Lorenz system:

$$\begin{aligned} \dot{x} &= \sigma(y - x) \\ \dot{y} &= x(\rho - z) - y \\ \dot{z} &= xy - \beta z, \end{aligned} \quad (5)$$

where $\sigma = 10$, $\rho = 28$, and $\beta = 8/3$ produces chaotic behavior. Only the first state $x(k)$ with $\Delta t = 0.1$ is observed. Table 1 lists the hyperparameters used to train the ESN. The performance of an ESN with and without delay embedding is depicted in Fig. 3. Fig. 4 provides a detailed error profile for different embedding dimensions m . The normalized mean absolute error (NMAE) between true and predicted scalar value ($x(k)$ and $\hat{x}(k)$ resp.) is given by $|x(k) - \hat{x}(k)|/|x(k)|$ and plotted with time in Fig. 4(a) for $m = 1$ and 5. The normalized root mean square error (NRMSE) between the true sequence $\{x(i) : i = 1, \dots, l\}$ and the predicted sequence $\{\hat{x}(i) : i = 1, \dots, l\}$ is given by

$$\text{NRMSE}(x, \hat{x}) = \sqrt{\frac{\sum_{i=1}^l \|x(i) - \hat{x}(i)\|^2}{\sum_{i=1}^l \|x(i)\|^2}}, \quad (6)$$

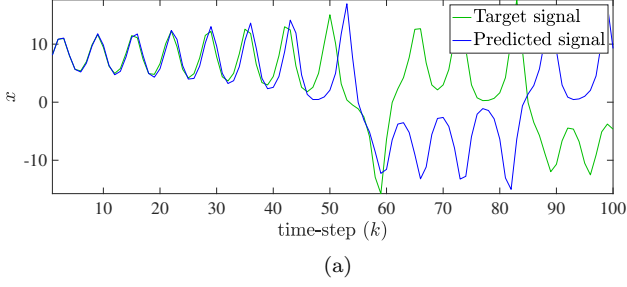
where l is the prediction length. The prediction NRMSEs for different delay embeddings over 50 independent Monte-Carlo trials are plotted in Fig. 4(b). As we can see, the error median is lowest with $m = 5$ as predicted by Taken's theorem.

4.2 Rössler System

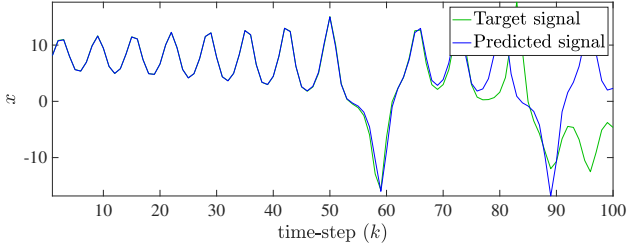
Next, the delay-embedded ESN is utilized to predict the partial state measurement generated by the Rössler system described in Rössler (1976):

$$\begin{aligned} \dot{x} &= -y - x \\ \dot{y} &= x + ay \\ \dot{z} &= b + z(x - c), \end{aligned} \quad (7)$$

with $a = 0.5$, $b = 2$, and $c = 4$ to produce chaotic behavior. Similar to the Lorenz system example, only $x(k)$ with $\Delta t = 0.1$ is observed. Table 1 lists the hyperparameters used to train the ESN. The performance of an ESN with and without delay embedding is depicted in Fig. 5. Fig. 6(a) provides a the normalized MAE with time with different values of the embedding dimension m . Fig. 6(b) plots the overall NRMSE for different m . Here also, $m = 5$ yields the best performance and almost an order of magnitude improvement in error than its counterpart with no delay embedding, i.e., $m = 1$. The results are generated by 50 independent Monte-Carlo trials for training and testing the ESNs.

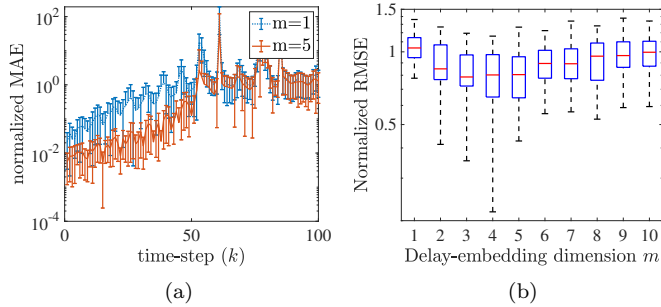


(a)



(b)

Fig. 3. Estimation of the partially observed time-series $x(k)$ from Lorenz system (5) (a) true and estimated signal with no delay embedding ($m = 1$), (b) true and estimated signal with 5 dimensional delay embedding ($m = 5$)



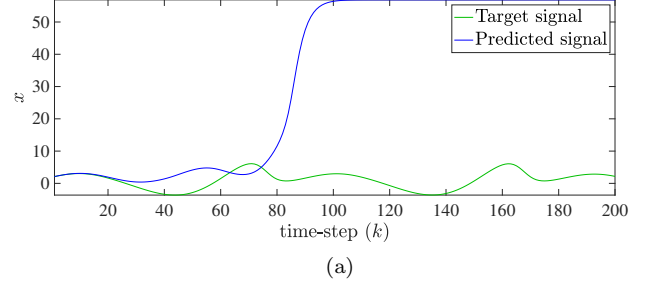
(a)

(b)

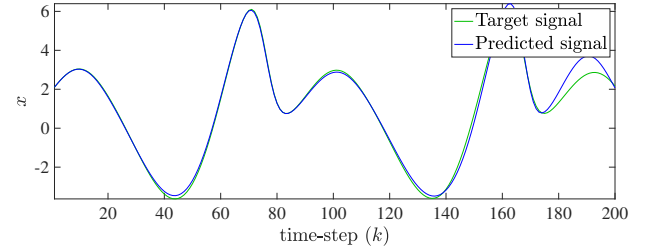
Fig. 4. Error profile of partially observed Lorenz time-series estimation: (a) NMAE with time for different embedding dimension m , (b) NRMSE with different embedding dimension m

4.3 Prediction of Traffic Volume on an Intersection of a Road Network

The proposed method is now applied to a dataset of traffic volumes obtained from Numina (Numina (2019)) sensors at five different intersections on the University of Maryland campus. Fig. 7(a) represents the road network marked with sensor locations. Each sensor counts the number of pedestrians, bicycles, and vehicles at the respective intersections and store them in a server. We use the time series data of hourly vehicle traffic volume for two months. The ESN is trained on 1000 hours of traffic volume data and tested for one week, i.e., 168 hours. During each training, data from only one sensor is used. The training hyperparameters are listed in Table 1. Fig. 8 shows the traffic volume prediction with delay embedding dimension of $m = 10$ and $m = 100$. Fig. 9 shows the NRMSE and Pearson correlation coefficient between

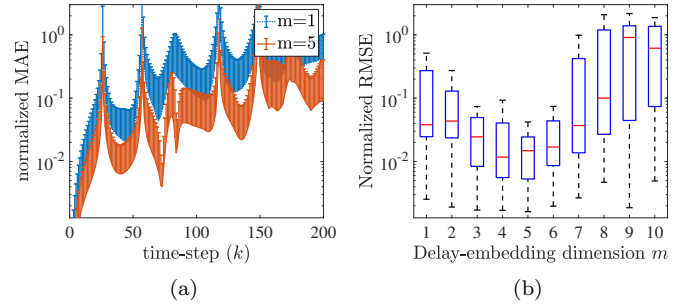


(a)



(b)

Fig. 5. Estimation of the partially observed time-series $x(k)$ from Rössler system (7): (a) true and estimated signal with no delay embedding ($m = 1$), (b) true and estimated signal with 5 dimensional delay embedding ($m = 5$)



(a)

(b)

Fig. 6. Error profile of partially observed Rössler time-series estimation: (a) NMAE with time, (b) NRMSE with different embedding dimension m

predicted and true traffic volumes with sensor data from different intersections. The Pearson correlation coefficient between true and predicted sequences ($\{x(i) : i = 1, \dots, l\}$ and $\{\hat{x}(i) : i = 1, \dots, l\}$ respectively) measures their normalized linear correlation. It is given by

$$r(x, \hat{x}) = \frac{\sum_i (x(i) - \bar{x})^T (\hat{x}(i) - \bar{\hat{x}})}{\sqrt{\sum_i \|x(i) - \bar{x}\|^2} \sqrt{\sum_i \|\hat{x}(i) - \bar{\hat{x}}\|^2}}, \quad (8)$$

where \bar{x} and $\bar{\hat{x}}$ denotes the time-average values of $x(i)$ and $\hat{x}(i)$. The performance of the ESN increases significantly with increasing embedding dimension m .

Remark 7. This example proves that delay embedding can significantly improve an ESN's predictive power for quasiperiodic partial state data coming from a very high-dimensional system. Here, the traffic volume can be thought as a spatio-temporal dynamical system evolving over the road-network.

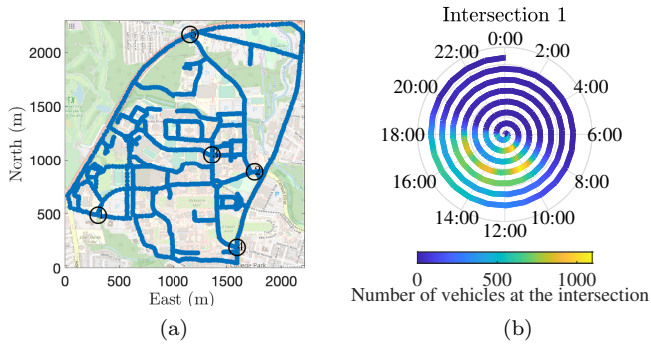


Fig. 7. Schematic diagram of traffic data: (a) University of Maryland road network with Numina sensors, (b) Traffic congestion pattern of an intersection over a single week, each revolution denotes a day of the week with times marked as angles; the number of vehicles is denoted by the colormap. The daily pattern of peak congestion between mornings and afternoons is evident.

5. CONCLUSION

This paper describes a data-driven prediction method for partially observed systems and uses it to estimate the partial state measurements of three nonlinear systems from time-series data. The method utilizes the echo-state network (ESN) and Taken's embedding theorem for model identification using time-delay embedded partial state measurements. The prediction is carried out in a data-driven fashion without a dynamic model. The method is applied to a real data set of traffic patterns on the road network of the University of Maryland, College Park campus to predict the traffic volume at various intersections. In ongoing and future work, inference of unobserved states via time-delay embedded ESN with surrogate spatial interpolation model and a data-driven controller design will be investigated.

ACKNOWLEDGEMENTS

The author thanks Dr. Derek A. Paley and the University of Maryland Department of Transportation for the Numina sensor data. The author also thanks Dr. Artur Wolek for preprocessing the data.

REFERENCES

Chen, J., Nurdin, H.I., and Yamamoto, N. (2019). Towards single-input single-output nonlinear system identification and signal processing on near-term quantum computers. In *2019 IEEE 58th Conference on Decision and Control (CDC)*, 401–406.

Fawzi, A., Balog, M., Huang, A., Hubert, T., Romera-Paredes, B., Barekatin, M., Novikov, A., R. Ruiz, F.J., Schrittwieser, J., Swirszcz, G., Silver, D., Hassabis, D., and Kohli, P. (2022). Discovering faster matrix multiplication algorithms with reinforcement learning. *Nature*, 610(7930), 47–53.

Fujii, K. and Nakajima, K. (2017). Harnessing disordered-ensemble quantum dynamics for machine learning. *Phys. Rev. Applied*, 8, 024030.

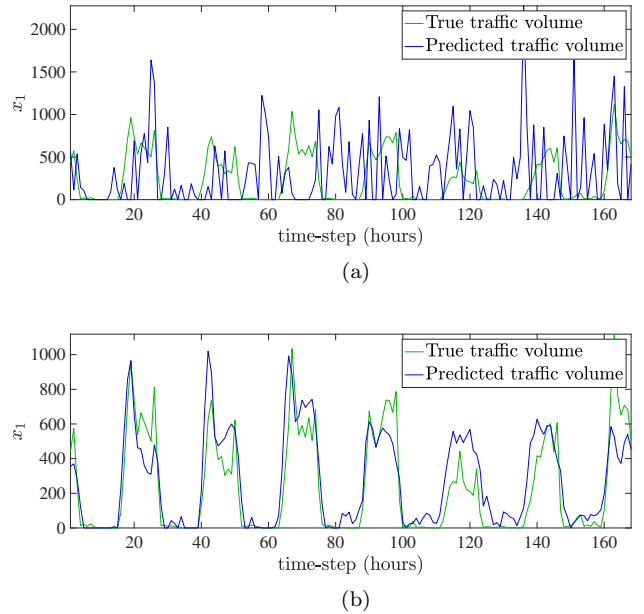


Fig. 8. Estimation of the partially observed traffic-volume time-series recorded from the Numina sensor at intersection 1: (a) true and estimated traffic volume with 10 dimensional delay embedding ($m = 10$), (b) true and estimated traffic volume with 100 dimensional delay embedding ($m = 100$)

Goswami, D., Riggins, A., and Paley, D.A. (2022). Data-driven prediction of urban micromobility: A study of dockless electric scooters [applications of control]. *IEEE Control Systems Magazine*, 42(5), 18–31.

Goswami, D., Wolek, A., and Paley, D.A. (2021). Data-driven estimation using an echo-state neural network equipped with an ensemble kalman filter. In *2021 American Control Conference (ACC)*, 2549–2554.

Grigoryeva, L. and Ortega, J.P. (2018). Echo state networks are universal. *Neural Networks*, 108, 495 – 508.

Hinton, G., Deng, L., Yu, D., Dahl, G.E., Mohamed, A., Jaitly, N., Senior, A., Vanhoucke, V., Nguyen, P., Sainath, T.N., and Kingsbury, B. (2012). Deep neural networks for acoustic modeling in speech recognition: The shared views of four research groups. *IEEE Signal Processing Magazine*, 29(6), 82–97.

Jaeger, H. and Haas, H. (2004). Harnessing nonlinearity: Predicting chaotic systems and saving energy in wireless communication. *Science*, 304(5667), 78–80.

Lu, Z., Pathak, J., Hunt, B., Girvan, M., Brockett, R., and Ott, E. (2017). Reservoir observers: Model-free inference of unmeasured variables in chaotic systems. *Chaos: An Interdisciplinary Journal of Nonlinear Science*, 27(4), 1054–1500.

Maass, W. and Markram, H. (2004). On the computational power of circuits of spiking neurons. *Journal of Computer and System Sciences*, 69(4), 593 – 616.

Nakajima, K. and Fischer, I. (2021). *Reservoir Computing: Theory, Physical Implementations, and Applications*. Springer Singapore, Singapore.

Nijmeijer, H. (1982). Observability of autonomous discrete time non-linear systems: a geometric approach. *International Journal of Control*, 36(5), 867–874.

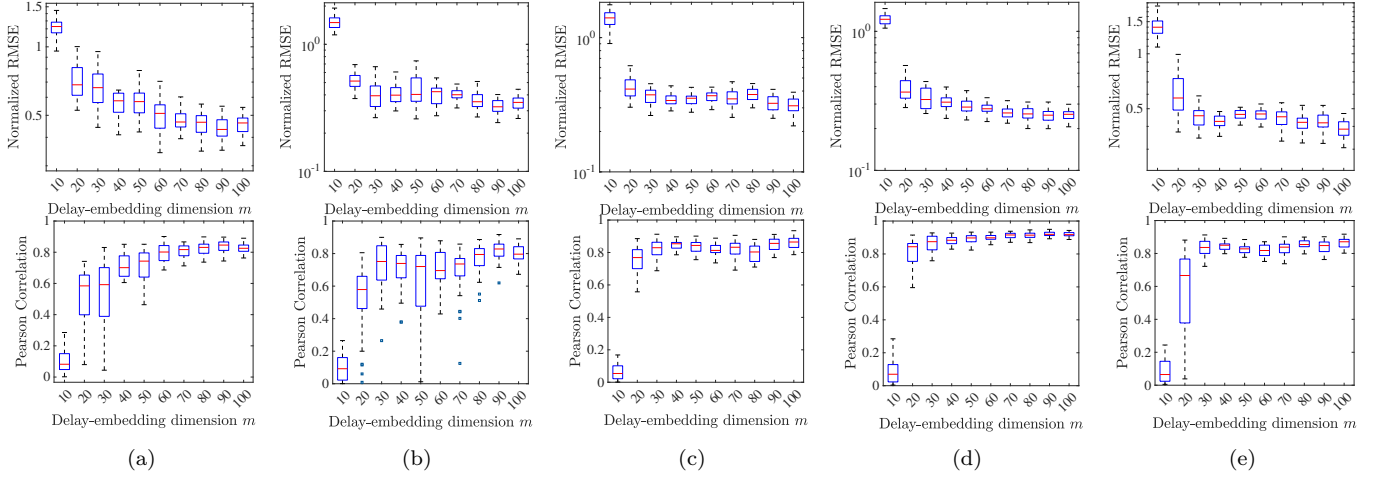


Fig. 9. NRMSE and Pearson correlation coefficient with different embedding dimensions m : (a) Intersection 1, (b) Intersection 2, (c) Intersection 3, (d) Intersection 4, (e) Intersection 5

Numina (2019). Numina mobility solutions. <https://numina.co>.

Pathak, J., Hunt, B., Girvan, M., Lu, Z., and Ott, E. (2018). Model-free prediction of large spatiotemporally chaotic systems from data: A reservoir computing approach. *Phys. Rev. Lett.*, 120, 024102.

Rössler, O. (1976). An equation for continuous chaos. *Physics Letters A*, 57(5), 397–398.

Sauer, T., Yorke, J.A., and Casdagli, M. (1991). Embedology. *Journal of Statistical Physics*, 65(3), 579–616.

Silver, D., Huang, A., Maddison, C.J., Guez, A., Sifre, L., van den Driessche, G., Schrittwieser, J., Antonoglou, I., Panneershelvam, V., Lanctot, M., Dieleman, S., Grewe, D., Nham, J., Kalchbrenner, N., Sutskever, I., Lillicrap, T., Leach, M., Kavukcuoglu, K., Graepel, T., and Hassabis, D. (2016). Mastering the game of Go with deep neural networks and tree search. *Nature*, 529(7587), 484–489.

Takens, F. (1981). Detecting strange attractors in turbulence. In D. Rand and L.S. Young (eds.), *Dynamical Systems and Turbulence, Warwick 1980*, 366–381. Springer Berlin Heidelberg, Berlin, Heidelberg.

Tanaka, G., Yamane, T., Héroux, J.B., Nakane, R., Kanazawa, N., Takeda, S., Numata, H., Nakano, D., and Hirose, A. (2019). Recent advances in physical reservoir computing: A review. *Neural Networks*, 115, 100–123.

Vlachos, I. and Kugiumtzis, D. (2008). State space reconstruction for multivariate time series prediction. *arXiv preprint arXiv:0809.2220*.

Appendix A. WHAT HAPPENS WITH UNOBSERVABLE SYSTEMS?

Consider the Lorenz system (5) with the observation $h([x, y, z]) = z$. This is an unobservable system since the system is invariant under the transformation $(x, y, z) \rightarrow (-x, -y, z)$, i.e., two different initial conditions on the strange attractor can produce the same observation data. In this case, it is shown in Fig. A.1 that the delay embedding does not significantly improve the prediction accuracy of the ESN.

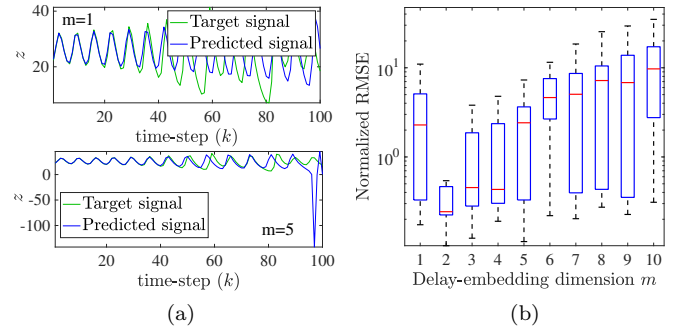


Fig. A.1. Estimation of the partially observed time-series $z(k)$ from Lorenz system (5): (a) true and estimated signal with no delay embedding ($m = 1$) and 5 dimensional delay embedding ($m = 5$), (b) NRMSE over 50 Monte-Carlo trials with different m . Delay embedding doesn't improve the performance over $m = 2$ due to unobservability.